



Corrosion and Dye

Elixir Corrosion & Dye 82 (2015) 32393-32402

Elixir
ISSN: 2229-712X

Metal-Organic Frameworks as Effective Inhibitors for the Corrosion of Low Carbon Steel in Aqueous Media

A.S. Fouda, S. Etaiw and S. Sobhy

Department of Chemistry, Tanta University, Tanta-35516, Egypt.

ARTICLE INFO

Article history:

Received: 8 April 2015;

Received in revised form:
30 April 2015;

Accepted: 6 May 2015;

Keywords

Corrosion inhibition,
C-steel,
HCl,
Metal-organic frameworks derivatives.

ABSTRACT

Inhibition of C-steel corrosion by metal-organic frameworks containing heterocyclic ligand of Ag (I) in 1 M HCl was investigated by weight loss, potentiodynamic polarization, electrochemical impedance spectroscopy (EIS) and electrochemical frequency modulation (EFM) measurements. The inhibition efficiency increased with increase in inhibitor concentration but decreased with rise in temperature. The thermodynamic parameters of corrosion and adsorption processes were determined and discussed. The adsorption of these inhibitors was found to obey Temkin's adsorption isotherm. Whereas thermodynamic suggested that a physisorption process occurred. The surface morphology of carbon steel sample was investigated by scanning electron microscopy (SEM).

© 2015 Elixir All rights reserved.

Introduction

Corrosion inhibitors are widely used in the industry to prevent or reduce the corrosion rates of metallic materials in acid media [1, 2]. Hydrochloric acid solutions are widely used for acid clearing, industry cleaning etc. Therefore, corrosion inhibitors for metals in hydrochloric acid have attracted more attention because of its wide application [3-8]. Compounds with nitrogen and oxygen function group as well as multiple bonds or aromatic rings are considered to be one of the most effective chemicals for inhibiting the corrosion of metals [9-11]. Though many synthetic compounds have shown good anticorrosive activity, most of them are highly toxic to both human beings and environment. The safety and environmental issues of corrosion inhibitors arisen in industries has always been a global concern. Such inhibitors may cause reversible (temporary) or irreversible (permanent) damage to organ system viz., kidneys or liver, or to disturb a biochemical process or to disturb an enzyme system at some sites in the human body.

The corrosion inhibition efficiency of organic compounds is related to their adsorption properties. Adsorption depends on the nature and the state of the metal surface, on the type of corrosive medium and on the chemical structure of the inhibitor [12]. Studies report that the adsorption of the organic inhibitors mainly depends on some physico-chemical properties of the molecule related to its functional group, to the possible steric effects and electronic density of donor atoms; adsorption is also supposed to depend on the possible interaction of π -orbital of the inhibitor with d-orbital of the surface atoms, which induce greater adsorption of the inhibitor molecules onto the surface of C-steel, leading to the formation of corrosion protecting film [13,14]. The present work was designed to study the corrosion inhibition of C-steel in 1M HCl solutions by some Metal-organic frameworks as corrosion inhibitors using weight loss, different electrochemical techniques, also, to compare the experimental results with the theoretical ones.

Experimental methods

Materials and solutions

The working electrode was mechanically cut from cylindrical carbon steel rod having composition (weight %): C 0.2; Mn 0.9; P 0.007; Si 0.002 % and the rest Fe) of rectangular design having an area of 1 cm² were used in this study. The surface of working electrode was abraded using different grades (320–1200 grade) of emery papers, degreased with acetone, washed with distilled water and dried with soft paper. The experimental measurements were carried out in 1 M HCl solution in the absence and presence of various concentrations of metal carbon frameworks derivatives for all studies. The chemical structure of metal organic frameworks derivatives is given in Table 1. In this study, the metal carbon frameworks derivatives presented in Table 1, which is tested as corrosion inhibitor was synthesized according to our used and known experimental methods [15]. The concentrations of inhibitors employed were varied as (1x 10⁻⁶M, 5 x 10⁻⁶ M, 1x10⁻⁵M, 5X10⁻⁵M, 1X10⁻⁴M). For each experiment, a freshly prepared solution was used. Table 1 shows the structures, molecular weights and molecular formulas of these compounds.

Weight loss tests

C- steel sheets of 20 x 20 x 2 mm were abraded with different grades of emery paper up to 1200 grit and then washed with bidistilled water and acetone. After weighing accurately, the specimens were immersed in 100 ml HCl solution with and without addition of different concentrations of inhibitors. After 3 hrs, the specimens were taken out, washed, dried, and weighed accurately. The average weight loss of the three parallel C- steel sheets could be obtained at required temperature. The inhibition efficiency (IE) and the degree of surface coverage (θ) of the investigated inhibitors were calculated as follows [16]:

$$\%IE = \theta \times 100 = [1 - (W / W^{\circ})] \times 100 \quad (1)$$

Where W[°] and W are the values of the average weight loss without and with addition of the inhibitor, respectively.

Electrochemical Measurements

Potentiodynamic polarization measurements

Polarization experiments were carried out in a conventional three-electrode cell with platinum gauze as auxiliary electrode and a saturated calomel electrode (SCE) coupled to a fine Luggin capillary as reference electrode. The working electrode was in the form of a square cut from C-steel sheet of equal composition embedded in epoxy resin of polytetrafluoroethylene so that the flat surface area was 1 cm². Prior to each measurement, the electrode surface was pretreated in the same manner as in the weight loss experiments. Before measurements, the electrode was immersed in solution for 30 min until a steady state was reached. The potential was started from - 600 to + 400 mV vs open circuit potential (E_{ocp}). All experiments were carried out in freshly prepared solutions at 25°C and results were always repeated at least three times to check the reproducibility. Then i_{corr} was used for the calculation of inhibition efficiency and surface coverage (θ) as follows:

$$\%IE = \theta \times 100 = (1 - (i_{corr}/i_{corr}^{\circ})) \times 100 \quad (2)$$

Where i_{corr}° and i_{corr} are corrosion current densities in the absence and presence of inhibitor, respectively.

Electrochemical impedance spectroscopy (EIS) measurements

Impedance measurements were carried out using AC signals of 5 mV peak to peak amplitude at the open circuit potential in the frequency range of 100 kHz to 0.1 Hz. All impedance data were fitted to appropriate equivalent circuit using the Gamry Echem Analyst software version 6.03.

Electrochemical frequency modulation technique

EFM experiments were performed with applying potential perturbation signal with amplitude 10 mV with two sine waves of 2 and 5 Hz. The choice for the frequencies of 2 and 5 Hz was based on three arguments [17-19]. The larger peaks were used to calculate the corrosion current density (i_{corr}), the Tafel slopes (β_c and β_a) and the causality factors CF-2 and CF-3 [20]. The electrode potential was allowed to stabilize for 30 min before starting the measurements. All the experiments were conducted at 25°C. Measurements were performed using Gamry Instrument Potentiostat/ Galvanostat/ ZRA (PCI4-G750). Gamry applications include DC105 software for DC corrosion measurements, EIS300 software for electrochemical impedance spectroscopy (EIS) measurements and EFM140 for electrochemical frequency modulation (EFM) measurements along with a computer for collecting data. Echem analyst v 6.03 software was used for plotting, graphing, and fitting data.

Scanning Electron Microscopy (SEM) Measurements

The electrode surface of C-steel was examined by scanning electron microscope – type JOEL 840, Japan before and after immersion in 1 M HCl test solution in the absence and in presence of the optimum concentrations of the investigated inhibitors at 25°C, for 1 day immersion time. The specimens were washed gently with bidistilled water, then dried carefully and examined without any further treatments.

Results and Discussion

Chemical Method (Weight-loss measurements)

Weight-loss of C-steel was determined, at various time intervals, in the absence and presence of different concentrations of metal carbon frameworks derivatives (1 and 2). The obtained weight-loss time curves are represented in Figure 1 for inhibitor (1), the most effective one. Similar curves were obtained for the other inhibitor (not shown). The inhibition efficiency of corrosion was found to be dependent on the inhibitor concentrations. The curves obtained in the presence of inhibitors fall significantly below that of free acid. In all cases, the increase

in the inhibitor concentration was accompanied by a decrease in weight-loss and an increase in the percentage inhibition. These results lead to the conclusion that these compounds are fairly efficient as inhibitors for C-steel dissolution in hydrochloric acid solution. Also, the degree of surface coverage (θ) was increased by increasing the inhibitor concentration. In order to get a comparative view, the variation of the percentage inhibition (%IE) of the two inhibitors with their molar concentrations determined. The values obtained are summarized in Table 2. Careful inspection of these results showed that, at the same inhibitor concentration, the order of inhibition efficiency is as follows: 1>2.

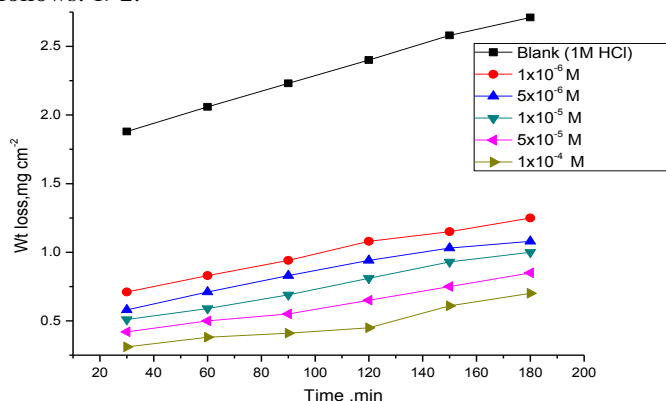


Figure 1. Weight loss-time curves for the corrosion of C-steel in 1 M HCl in the absence and presence of different concentrations of inhibitor (1) at 25 °C

Effect of Temperature

The effect of temperature on the corrosion rate of C-steel in 1M HCl and in presence of different inhibitor concentrations was studied in the temperature range of 25-45°C using weight loss measurements. As the temperature increases, the rate of corrosion increases and the inhibition efficiency of the inhibitors decrease as shown in Table 3 for the two inhibitors. The adsorption behavior of inhibitors on carbon steel surface occurs through physical adsorption.

Adsorption Isotherms

One of the most convenient way of expressing adsorption quantitatively is by deriving the adsorption isotherm that characterize the metal/inhibitor/ environment system. Various adsorption isotherms were applied to fit θ values but the best fit was found to obey Temkin's adsorption isotherm which are represented in Figure 2 for inhibitors, Temkin's adsorption isotherm may be expressed by:

$$a\theta = \ln K C \quad (3)$$

Where C is the concentration (mol L⁻¹) of the inhibitor in the bulk electrolyte, θ is the degree of surface coverage ($\theta = \%IE/100$), K_{ads} is the adsorption equilibrium constant. A plot of θ versus $\log C$ should give straight lines with slope equals $2.303/a$ and intercept equals $(2.303/a \log K)$. The experimental data give good curves fitting for the applied adsorption isotherm as the correlation coefficients (R^2) were in the range (0.953-0.999). The values obtained are given in Table 4. These results confirm the assumption that, these compounds are adsorbed on the metal surface through the lone pair of electrons of N and O atoms. The extent of inhibition is directly related to the performance of adsorption layer which is a sensitive function of the molecular structure. The equilibrium constant of adsorption K_{ads} obtained from the intercepts of Temkin adsorption isotherm is related to the free energy of adsorption ΔG°_{ads} as follows:

$$K_{ads} = 1/55.5 \exp [-\Delta G^{\circ}_{ads} / RT]$$

Where, 55.5 is the molar concentration of water in the solution in M^{-1}

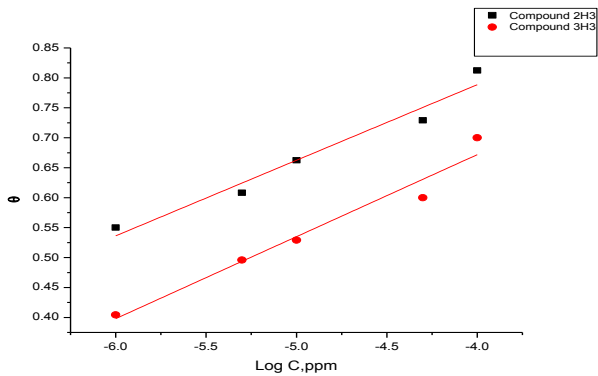


Figure 2. Temkin adsorption isotherm of inhibitors on C-steel in 1 M HCl at 25°C

Plot of (ΔG_{ads}°) versus T Figure 3 gave the heat of adsorption (ΔH_{ads}°) and the standard entropy (ΔS_{ads}°) according to the thermodynamic basic equation 4:

$$\Delta G_{ads}^{\circ} = \Delta H_{ads}^{\circ} - T \Delta S_{ads}^{\circ} \quad (4)$$

Table 5 clearly shows a good dependence of ΔG_{ads}° on T , indicating the good correlation among thermodynamic parameters. The negative value of ΔG_{ads}° reflects that the adsorption of studied inhibitors on C-steel surface in 1M HCl solution is spontaneous process and stability of the adsorbed layer on the carbon steel surface. Generally, values of ΔG_{ads}° around -20 kJ mol^{-1} or lower are consistent with the electrostatic interaction between the charged molecules and the charged metal (physical adsorption); those around -40 kJ mol^{-1} or higher involves charge sharing or transfer from organic molecules to the metal surface to form a coordinate type of bond (chemisorptions) [21]. From the obtained values of ΔG_{ads}° it was indicated that these compounds are adsorbed on carbon steel surface physically. The unshared electron pairs in oxygen, nitrogen may interact with d-orbital of C-steel to provide a protective physical adsorbed film [22]. The values of thermodynamic parameter for the adsorption of inhibitors Table 5 can provide valuable information about the mechanism of corrosion inhibition. In the presented case, the calculated values of ΔH_{ads}° for the adsorption of inhibitors in 1 M HCl indicate that these inhibitors may be endothermically adsorbed. The values of ΔS_{ads}° in the presence of inhibitors are negative that is accompanied with endothermic adsorption process. This indicates that an increase in disorder takes places on going from reactants to the metal-adsorbed reaction complex [23].

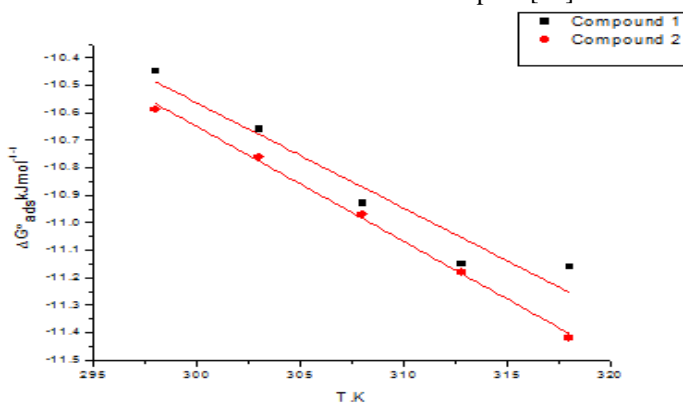


Figure 3. Variation of ΔG_{ads}° versus T for the adsorption of inhibitors on C-steel surface in 1 M HCl at different temperatures

Kinetic –Thermodynamic Corrosion Parameters

The effect of temperature on both corrosion and corrosion inhibition of carbon steel in 1 M HCl solution in the absence and presence of different concentrations of investigated compounds at different temperatures was studied using weight loss measurements. The corrosion rate increases with increasing temperature both in uninhibited and inhibited acid. The apparent activation energy (E_a^*) for the corrosion process can be calculated from Arrhenius-type equation (5):

$$k_{corr} = A \exp(E_a^*/RT) \quad (5)$$

Where (E_a^*) is the apparent activation corrosion energy, R is the universal gas constant, T is the absolute temperature and A is the Arrhenius pre-exponential constant. Values of apparent activation energy of corrosion for C-steel in 1 M HCl ($E_a^* = (\text{slope}) 2.303 \times R$) without and with various concentrations of investigated compounds are shown in Table 6. Plots of $\log(k_{corr})$ versus $1/T$ are shown in Figure 4 for compound (1). Inspection of the data shows that the activation energy is lower in the presence of inhibitors than in its absence. This was attributed to slow rate of inhibitor adsorption with a resultant closer approach to equilibrium during the experiments at higher temperatures according to Hoar and Holliday [24]. But, Riggs and Hurd [25] explained that the decrease in the activation energy of corrosion at higher levels of inhibition arises from a shift of the net corrosion reaction from the uncovered part of the metal surface to the covered one. Schmid and Huang [26] found that organic molecules inhibit both the anodic and cathodic partial reactions on the electrode surface and a parallel reaction takes place on the covered area, but the reaction rate on the covered area is substantially less than on the uncovered area similar to the present study. The alternative formulation of transition state equation is shown in Eq. (6):

$$k_{corr} = (RT/h) \exp(\Delta S^*/R) \exp(-\Delta H^*/RT) \quad (6)$$

Where k_{corr} is the rate of metal dissolution, h is Planck's constant, N is Avogadro's number, ΔS^* is the entropy of activation and ΔH^* is the enthalpy of activation. Figure 6 shows a plot of $\log(k/T)$ against $(1/T)$ in the case of inhibitor (1) in 1 M HCl. Similar behavior is observed in the case of inhibitor 2 (not shown). Straight lines are obtained with a slopes equal to $(\Delta H^*/2.303R)$ and intercepts are $[\log(R/h) + \Delta S^*/2.303R]$ are calculated Table 5.

The increase in E_a^* with increase inhibitor concentration Table 6 is typical of physical adsorption. The positive signs of the enthalpies (ΔH^*) reflect the endothermic nature of the C-steel dissolution process. Value of entropies (ΔS^*) imply that the activated complex at the rate determining step represents an association rather than a dissociation step, meaning that a decrease in disordering takes place on going from reactants to the activated complex [27, 28]. However, the value of (ΔS^*) decreases gradually with increasing inhibitor concentrations in all the acid media .

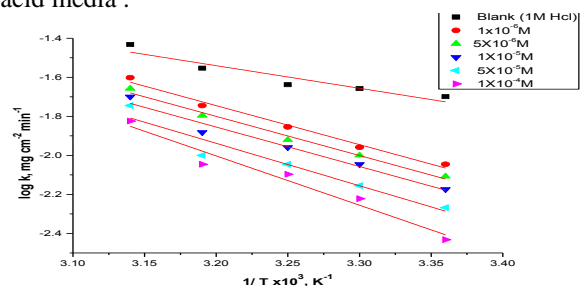


Figure 4. Log k vs. $(1/T)$ curves for Arrhenius plots for C-steel corrosion rates (k_{corr}) after 120 minute of immersion in 1M HCl in the absence and presence of various concentrations of inhibitor (1)

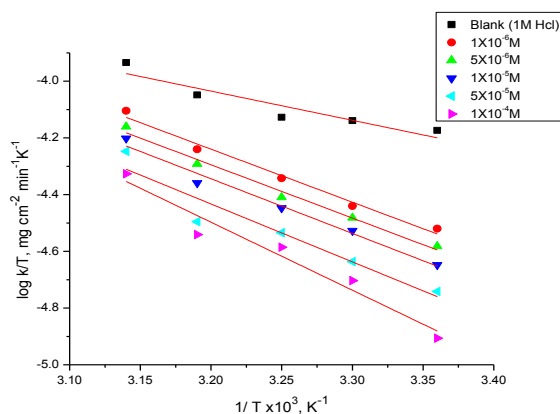


Figure 5. Log (k_{corr}/T) vs. ($1/T$) curves for Transition plots for C-steel corrosion rates (k_{corr}) after 120 minute of immersion in 1M HCl in the absence and presence of various concentrations of inhibitor (1)

Potentiodynamic Polarization Measurements

Figure 6 shows typical polarization curves for C-steel in 1 M HCl media. The two distinct regions that appeared were the active dissolution region (apparent Tafel region), and the limiting current region. In the inhibitor-free solution, the anodic polarization curve of C-steel showed a monotonic increase of current with potential until the current reached the maximum value. After this maximum current density value, the current density declined rapidly with potential increase, forming an anodic current peak. In the presence of inhibitor, both the cathodic and anodic current densities were greatly decreased over a wide potential range.

Various corrosion parameters such as corrosion potential (E_{corr}), anodic and cathodic Tafel slopes (β_a , β_c), the corrosion current density (i_{corr}), the degree of surface coverage (θ) and the inhibition efficiency (%IE) are given in Table 7.

It can see from the experimental results that in all cases, addition of inhibitors induced a significant decrease in cathode and anodic currents. The values of E_{corr} were affected and slightly changed by the addition of inhibitors. This indicates that these inhibitors act as mixed-type inhibitors. The slopes of anodic and cathodic Tafel lines (β_a and β_c), were slightly changed (Tafel lines are parallel); on increasing the concentration of the tested compounds which indicates that there is no change of the mechanism of inhibition in the presence and absence of inhibitors. The orders of inhibition efficiency of all inhibitors at different concentrations as given by polarization measurements are listed in Table 7. The results are in good agreement with those obtained from weight-loss measurements.

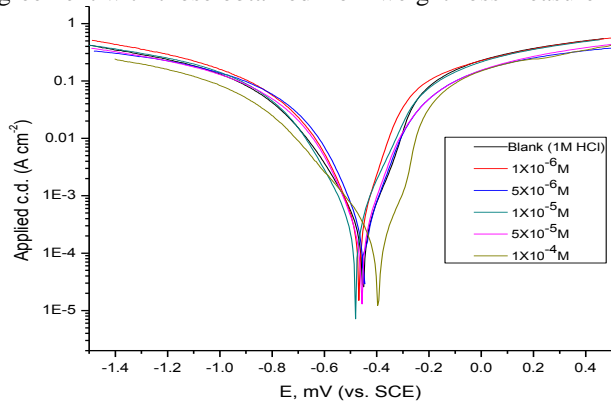


Figure 6. Potentiodynamic polarization curves for the dissolution of C-steel in 1M HCl in the absence and presence of different concentrations of compound (1) at 25°C

Electrochemical Impedance Spectroscopy (EIS) Measurements

EIS is well-established and it is powerful technique for studying the corrosion. Surface properties, electrode kinetics and mechanistic information can be obtained from impedance diagrams [29, 33]. Figure 8 shows the Nyquist (a) and Bode (b) plots obtained at open-circuit potential both in the absence and presence of increasing concentrations of investigated compounds at 25°C. The increase in the size of the capacitive loop with the addition of investigated compounds shows that a barrier gradually forms on the C-steel surface. The increase in the capacitive loop size (Figure 8a) enhances, at a fixed inhibitor concentration, following the order: (1) > (2), confirming the highest inhibitive influence of compound (1). Bode plots (Figure 8b), shows that the total impedance increases with increasing inhibitor concentration ($\log Z$ vs. $\log f$). But ($\log f$ vs. phase), also Bode plot shows the continuous increase in the phase angle shift, obviously correlating with the increase of inhibitor adsorbed on C-steel surface. The Nyquist plots do not yield perfect semicircles as expected from the theory of EIS. The deviation from ideal semicircle was generally attributed to the frequency dispersion [34] as well as to the heterogeneities of the surface.

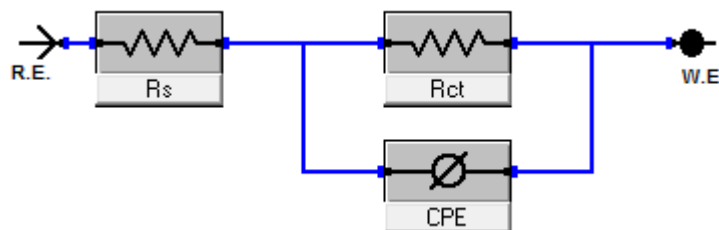


Figure 7. Equivalent circuit model used to fit experimental EIS

EIS spectra of the investigated compounds were analyzed using the equivalent circuit, Figure 7, which represents a single charge transfer reaction and fits well with our experimental results. The constant phase element, CPE, is introduced in the circuit instead of a pure double layer capacitor to give a more accurate fit [35]. The double layer capacitance, C_{dl} , for a circuit including a CPE parameter (Y_0 and n) were calculated from eq.7 [36]:

$$C_{\text{dl}} = Y_0 (\omega_{\text{max}})^{n-1} \quad (7)$$

where Y_0 is the magnitude of the CPE, $\omega_{\text{max}} = 2\pi f_{\text{max}}$, f_{max} is the frequency at which the imaginary component of the impedance is maximal and the factor n is an adjustable parameter that usually lies between 0.50 and 1.0. After analyzing the shape of the Nyquist plots, it is concluded that the curves approximated by a single capacitive semicircles, showing that the corrosion process was mainly charged-transfer controlled [37,38]. The general shape of the curves is very similar for all samples (in presence or absence of inhibitors at different immersion times) indicating that no change in the corrosion mechanism [39]. From the impedance data Table 8, we concluded that the value of R_{ct} increases with increasing the concentration of the inhibitors and this indicates an increase in % IE_{EIS}, which in concord with the EFM results obtained. In fact the presence of inhibitors enhances the value of R_{ct} in acidic solution. Values of double layer capacitance are also brought down to the maximum extent in the presence of inhibitor and the decrease in the values of CPE follows the order similar to that obtained for i_{corr} in this study. The decrease in CPE/ C_{dl} results from a decrease in local dielectric constant and/or an increase in the thickness of the double layer, suggesting that organic derivatives inhibit the C-steel corrosion by adsorption at

metal/acid [40, 41]. The inhibition efficiency was calculated from the charge transfer resistance data from eq.15 [42]:

$$\% IE_{EIS} = [1 - (R_{ct}^0 / R_{ct})] \times 100 \quad (8)$$

Where R_{ct}^0 and R_{ct} are the charge-transfer resistance values without and with inhibitor respectively

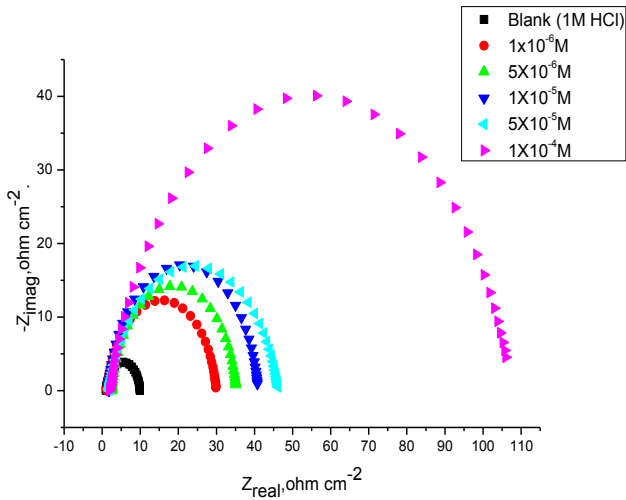


Figure 8a. The Nyquist plots for the corrosion of C-steel in 1M HCl in the absence and presence of different concentrations of inhibitor (1) at 25°C

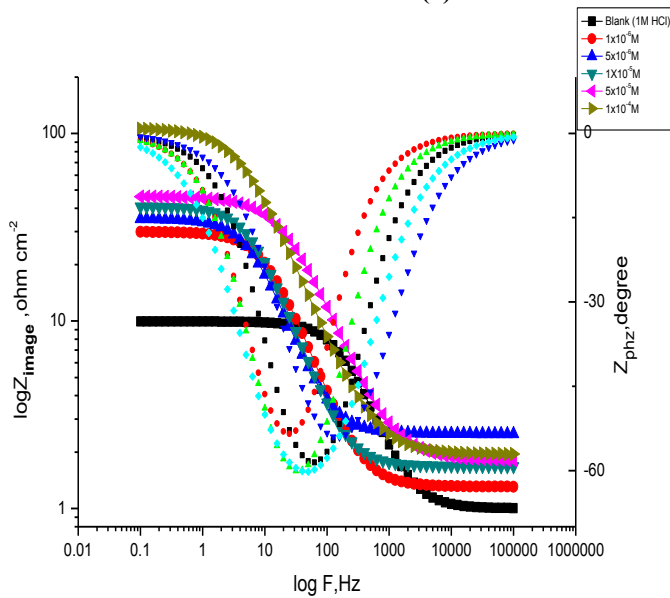


Figure 8b. The Bode plots for the corrosion of C-steel in 1M HCl in the absence and presence of different concentrations of inhibitor (1) at 25°C

Electrochemical Frequency Modulation (EFM) Measurements

EFM is a nondestructive corrosion measurement technique that can directly and quickly determine the corrosion current values without prior knowledge of Tafel slopes, and with only a small polarizing signal. These advantages of EFM technique make it an ideal candidate for online corrosion monitoring [43]. The great strength of the EFM is the causality factors which serve as an internal check on the validity of EFM measurement. The causality factors CF-2 and CF-3 are calculated from the frequency spectrum of the current responses. Figure 9 shows the EFM Inter modulation spectra (current vs. frequency) of C-steel in HCl solution containing different concentrations of compound (1). Similar curves were obtained for compound (2) (not shown). The harmonic and inter modulation peaks are clearly visible and are much larger than the background noise. The two large peaks, with amplitude of about 200 μ A, are the response to the 40 and

100 MHz (2 and 5 Hz) excitation frequencies. It is important to note that between the peaks there is nearly no current response (<100 nA). The experimental EFM data were treated using two different models: complete diffusion control of the cathodic reaction and the “activation” model. For the latter, a set of three non-linear equations had been solved, assuming that the corrosion potential does not change due to the polarization of the working electrode [44]. The larger peaks were used to calculate the corrosion current density (i_{corr}), the Tafel slopes (β_c and β_a) and the causality factors (CF-2 and CF-3). These electrochemical parameters were listed in Table 9. The data presented in Table 9 obviously show that, the addition of any one of tested compounds at a given concentration to the acidic solution decreases the corrosion current density, indicating that these compounds inhibit the corrosion of C-steel in 1 M HCl through adsorption. The causality factors obtained under different experimental conditions are approximately equal to the theoretical values (2 and 3) indicating that the measured data are verified and of good quality. The inhibition efficiencies $\% IE_{EFM}$ increase by increasing the inhibitor concentrations and was calculated as from Eq. (9):

$$\% IE_{EFM} = [1 - (i_{corr}^0 / i_{corr})] \times 100 \quad (9)$$

Where i_{corr}^0 and i_{corr} are corrosion current densities in the absence and presence of inhibitor, respectively. The inhibition sufficiency obtained from this method is in the order: (1) > (2).

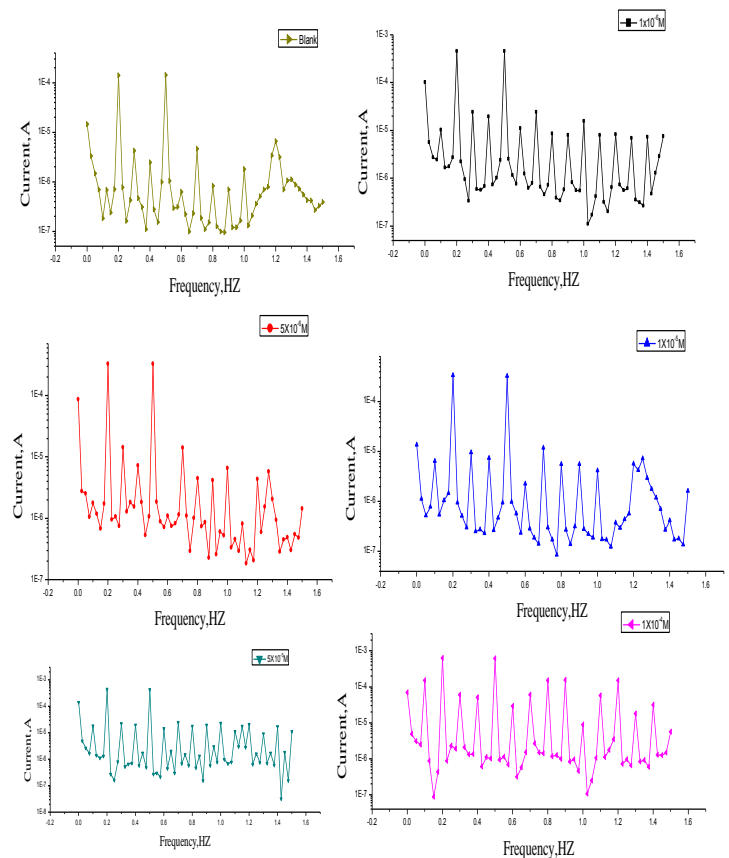


Figure 9. EFM spectra for C-steel in 1 M HCl in the absence and presence of different concentrations of compound (1) at 25°C

Surface Examinations

Scanning electron microscopy (SEM) and energy dispersive X-ray (EDX) experiments were carried out in order to verify if the investigated compounds are in fact adsorbed on C-steel surface or just peeled off the surface. SEM images were indicative of the changes that accompany both corrosion and protection of the carbon steel surface (Fig. 10a–f).

Table 1. Chemical structure of inhibitors

Inhibitor	Structures
1	
Mol.wt, Mol Formula	$C_{31}H_{37}N_4O_9Ag_2$, 824.6
2	
Mol.wt, Mol Formula	$C_{28}H_{20}N_4O_4Ag_2$, 691.612

Table 2. Data of weight loss measurements for carbon steel in 1 M HCl solution in the absence and presence of different concentrations of compound (1) at different temperatures

Temp, °C	[inh], M	Θ	% IE	CR
25	0.0	-	-	0.0200
	1×10^{-6}	0.550	55.0	0.0090
	5×10^{-6}	0.608	60.8	0.0078
	1×10^{-5}	0.663	66.3	0.0067
	5×10^{-5}	0.729	72.9	0.0054
	1×10^{-4}	0.813	81.3	0.0037
30	0.0	-	-	0.0220
	1×10^{-6}	0.508	50.8	0.0110
	5×10^{-6}	0.557	55.7	0.0100
	1×10^{-5}	0.610	61.0	0.0090
	5×10^{-5}	0.678	67.8	0.0070
	1×10^{-4}	0.720	72.0	0.0060
35	0.0	-	-	0.0230
	1×10^{-6}	0.411	41.1	0.0140
	5×10^{-6}	0.468	46.8	0.0120
	1×10^{-5}	0.538	53.8	0.0110
	5×10^{-5}	0.614	61.4	0.0090
	1×10^{-4}	0.664	66.4	0.0080
40	0.0	-	-	0.0280
	1×10^{-6}	0.362	36.2	0.0180
	5×10^{-6}	0.437	43.7	0.0160
	1×10^{-5}	0.506	50.6	0.0120
	5×10^{-5}	0.575	57.5	0.0100
	1×10^{-4}	0.638	63.8	0.0090
45	0.0	-	-	0.0370
	1×10^{-6}	0.306	30.6	0.0250
	5×10^{-6}	0.401	40.1	0.0220
	1×10^{-5}	0.466	46.6	0.0200
	5×10^{-5}	0.527	52.7	0.0180
	1×10^{-4}	0.606	60.6	0.0150

Table 3. Inhibition efficiency (%IE) of investigated compounds at different concentrations in 1 M HCl solution at different temperatures

Inhibitor	Concentration, M.	%IE				
		25°C	30°C	35°C	40°C	45°C
1	1×10^{-6}	55.0	50.8	41.1	36.2	30.6
	5×10^{-6}	60.8	55.7	46.8	43.7	40.1
	1×10^{-5}	66.3	61.0	53.8	50.6	46.6
	5×10^{-5}	72.9	67.8	61.4	57.5	52.7
	1×10^{-4}	81.3	72.0	66.4	63.8	60.6
2	1×10^{-6}	40.4	33.0	30.4	25.8	19.1
	5×10^{-6}	49.6	38.6	34.6	30.8	23.9
	1×10^{-5}	52.9	45.1	39.6	34.7	28.8
	5×10^{-5}	60.0	49.6	45.7	39.5	34.2
	1×10^{-4}	70.0	54.2	52.9	45.8	42.8

Table 4. Equilibrium constant (K_{ads}) of investigated compounds adsorbed on C-steel surface in 1M HCl at different temperatures

Inhibitor	Temperature °C	$K_{ads} \times 10^{-3} M^{-1}$	R^2	α
1	25	1.221	0.95	22.359
	30	1.241	0.98	21.523
	35	1.285	0.97	17.992
	40	1.306	0.98	16.934
	45	1.225	0.98	16.105
2	25	1.294	0.95	16.810
	30	1.289	0.97	21.726
	35	1.307	0.95	20.936
	40	1.308	0.96	23.990
	45	1.352	0.98	20.936

Table 5. Thermodynamic parameters for the adsorption of inhibitors on C-steel surface in 1M HCl at different temperatures

Inhibitor	Temp. °C	$K_{ads} \times 10^{-3} M^{-1}$	$-\Delta G^{\circ}_{ads} kJ mol^{-1}$	$\Delta H^{\circ}_{ads} kJ mol^{-1}$	$-\Delta S^{\circ}_{ads} J mol^{-1} K^{-1}$
1	25	1.22	10.45	73.1	35.065
	30	1.24	10.66		35.179
	35	1.29	10.93		35.485
	40	1.31	11.15		35.621
	45	1.23	11.16		35.065
2	25	1.294	10.59	78.5	35.534
	30	1.289	10.76		35.509
	35	1.307	10.97		35.614
	40	1.308	11.15		35.621
	45	1.352	11.42		35.910

Table 6. Activation parameters for C-steel corrosion in the absence and presence of various concentrations of inhibitors in 1M HCl

Inhibitor	[inh] M	$E_a^* kJ mol^{-1}$	$\Delta H^* kJ mol^{-1}$	$-\Delta S^* J mol^{-1} K^{-1}$	$A \times 10^7 g cm^{-2} min^{-1}$
Blank	0	22.17	19.71	211.65	0.015
1	1×10^{-6}	38.28	35.79	164.13	4.48
	5×10^{-6}	38.41	35.96	163.61	4.55
	1×10^{-5}	38.70	36.88	162.62	4.88
	5×10^{-5}	41.57	39.08	157.24	10.23
	1×10^{-4}	48.37	45.89	136.70	120.78
2	1×10^{-6}	34.7	32.43	173.10	1.52
	5×10^{-6}	35.73	33.26	171.32	1.87
	1×10^{-5}	38.16	35.69	164.22	4.42
	5×10^{-5}	39.77	37.30	159.65	7.57
	1×10^{-4}	44.13	41.64	146.88	35.40

Table 7. Corrosion potential (E_{corr}), corrosion current density (i_{corr}), Tafel slopes (β_c , β_a), degree of surface coverage (θ), and inhibition efficiency (% IE) of C-steel in 1M HCl at 25°C for inhibitors

Inh.	[inh] M	$-E_{corr} mV vs SCE$	$i_{corr} \mu A cm^{-2}$	$\beta_a mV dec^{-1}$	$\beta_c mV dec^{-1}$	C. R mpy	θ	% IE
Blank	0	428	550	91	155	251.3	-----	-----
1	1×10^{-6}	467	358	90	144	159.3	0.467	46.7
	5×10^{-6}	448	326	117	151	144.8	0.525	52.5
	1×10^{-5}	481	308	113	155	123.5	0.658	65.8
	5×10^{-5}	457	220	106	139	116.1	0.718	71.8
	1×10^{-4}	394	168	93	190	76.87	0.895	89.5
2	1×10^{-6}	504	547	64	133	70.81	0.440	44.0
	5×10^{-6}	501	414	68	128	152.1	0.507	50.7
	1×10^{-5}	513	406	68.6	114.3	134.8	0.562	56.2
	5×10^{-5}	500	388	65.5	110.8	120.7	0.659	65.9
	1×10^{-4}	495	308	68.1	125.5	112.8	0.740	74.0

Table 8. Electrochemical kinetic parameters obtained by EIS technique for in 1 M HCl without and with various concentrations of investigated compounds at 25°C

Concentration, M	R_p , $k\Omega\text{ cm}^2$	C_{dl} , $\mu\text{F cm}^{-2}$	θ	% IE	
1 M HCl	8.945	108.3	-----	---	
1	1×10^{-6}	28.62	83.6	0.588	58.8
	5×10^{-6}	32.71	68.3	0.626	62.6
	1×10^{-5}	39.22	52.1	0.672	67.2
	5×10^{-5}	44.47	17.3	0.709	70.9
	1×10^{-4}	105.5	15.3	0.815	81.5
2	1×10^{-6}	13.2	108.0	0.422	42.3
	5×10^{-6}	18.78	100.7	0.523	52.3
	1×10^{-5}	18.90	93.5	0.562	56.2
	5×10^{-5}	22.10	92.7	0.605	60.5
	1×10^{-4}	25.00	87.8	0.742	74.2

Table 9. Electrochemical kinetic parameters obtained from EFM technique for C-steel in 1M HCl in the absence and presence of different concentrations of investigated compounds

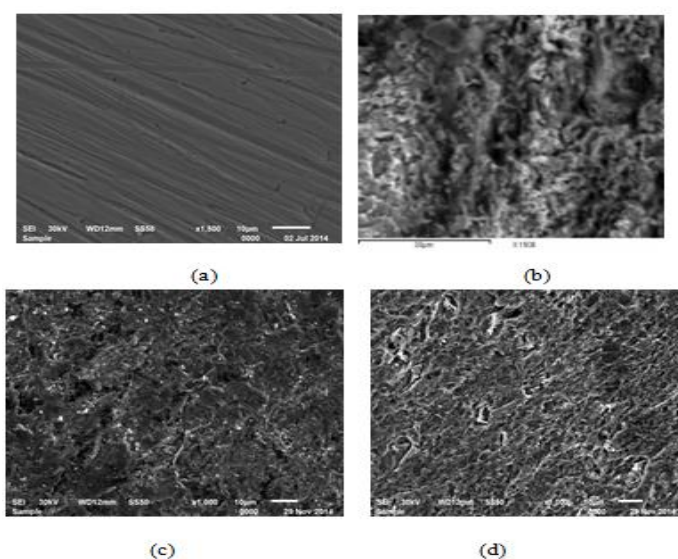
Inh	[inh] M	i_{corr} $\mu\text{A cm}^{-2}$	β_a mV dec^{-1}	β_c mV dec^{-1}	CF-2	CF-3	C.R mpy	Θ	% IE
Blank	0	595.5	74.59	98.71	1.375	2.994	272.3	-----	-----
1	1×10^{-6}	565.4	97.49	131.9	2.097	2.908	158.0	0.501	50.1
	5×10^{-6}	449.5	80.56	96.05	1.870	3.002	105.0	0.626	62.6
	1×10^{-5}	393.9	51.50	61.84	1.104	2.484	90.0	0.689	68.9
	5×10^{-5}	295.4	118.9	139.4	1.930	2.472	83.4	0.704	70.4
	1×10^{-4}	210.7	88.3	106.5	2.086	3.042	56.29	0.856	85.6
2	1×10^{-6}	559.7	71.30	85.63	1.357	2.725	165.7	0.461	46.1
	5×10^{-6}	362.5	45.33	47.00	1.847	2.798	155.6	0.512	51.2
	1×10^{-5}	301.6	36.32	36.57	1.814	2.986	137.8	0.564	56.4
	5×10^{-5}	301.0	34.96	37.75	1.641	3.001	107.6	0.635	63.5
	1×10^{-4}	245.5	26.09	27.85	1.565	3.898	82.2	0.728	72.8

Table 10. Surface composition (weight %) of C-steel after 1 day of immersion in 1 M HCl + 1×10^{-4} M of investigated inhibitors

Mass %	C	O	Ag	Fe
1	67.34	20.99	-----	11.67
2	71.11	20.84	0.80	7.25

Figure 10a shows the free metal. Figure 10b shows the damage caused to the surface by hydrochloric acid. Figure 10c, d shows SEM images of the carbon steel surface after treatment with 1 M HCl containing 1×10^{-4} M of investigated inhibitors. From these images, it is obvious that the steel surface seems to be almost unaffected by corrosion. This is because of adsorption of investigated inhibitors forming a thin protective film of the inhibitors on the metal surface. This film is responsible for the highly efficient inhibition by these inhibitors. The corresponding EDS profile analyses are presented in Table 10 and Figure 11 for investigated compounds. It is also important to notice the existence of C and O peaks in the EDS spectra of the C-steel surface corresponding to the samples immersed for 1 day in solutions containing the optimum concentration of these compounds. The formation of a thin inhibitor film is in agreement with the SEM observations.

The inhibition mechanism involves the adsorption of the inhibitor on the metal surface immersed in aqueous HCl solution. Four types of adsorption [45] may take place involving organic molecules at the metal-solution interface: 1) Electrostatic attraction between the charged molecules and the charged metal; 2) Interaction of unshared electron pairs in the molecule with the metal; 3) Interaction of π -electrons with the metal; 4) Combination of all the above.

**Figure 10. SEM micrographs of C-steel surface (a) before of immersion in 1 M HCl, (b) after 24 h of immersion in 1 M HCl, (c) after 24 h of immersion in 1 M HCl+ 1×10^{-4} M of compound 1, (d) after 24 h of immersion in 1 M HCl+ 1×10^{-4} M of compound 2 at 25°C**

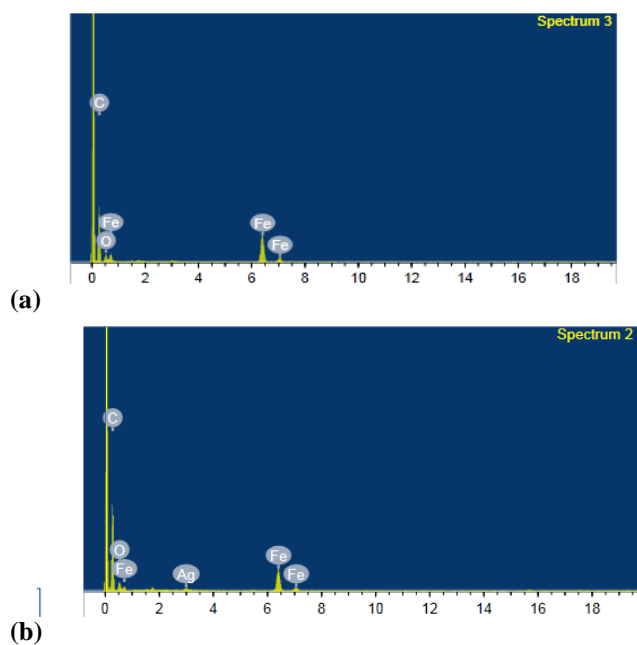


Figure 11. EDX spectra of C-steel in 1 M HCl in the presence of 1×10^{-4} M compound (1) (a), in 1×10^{-4} M compound (2) (b).

10 Mechanism of Corrosion Inhibition

From the observations drawn from the different methods, corrosion inhibition of C-steel in 1M HCl solutions by the investigated inhibitors as indicated from weight loss, potentiodynamic polarization and EIS techniques were found to depend on the concentration and the nature of the inhibitor. The order of inhibition efficiency is as follows: 1>2. The Metal organic frame works derivatives of the studied compounds contain polar groups such as oxygen and nitrogen. Each atom is a chemisorptions centre and the inhibition efficiency depends on the electron density around the chemisorptions center; higher the electron density at the chemisorptions centre, greater is the inhibition efficiency. The highest inhibition efficiency was observed for compound (1) as it has an additional Oxygen atom with lone pair of electrons. These electrons interact with the vacant d-orbital of Iron present in the C-steel surface and adsorb strongly there by blocking more number of adsorption sites on the C-steel surface. It has been previously reported in literature, that inhibiting effect depends mainly on inhibitor concentration, the molecular structure, size and structure of the side chain in the organic compounds. It is observed that, the inhibition efficiency of the Metal organic frame works derivatives increases with increase in concentration as a result of higher surface coverage in solutions containing higher concentration of inhibitors.

Conclusions

From the overall experimental results the following conclusions can be deduced:

1. The investigated compounds are good inhibitors and act as mixed type inhibitors for C-steel corrosion in 1 M HCl solution.
2. Reasonably good agreement was observed between the values obtained by the weight loss and electrochemical measurements were in good agreement. The order of % IE of these investigated compounds is in the following order: (1) > (2).
3. The results obtained from all electrochemical measurements showed that the inhibiting action increases with the inhibitor concentration and decreases with the increasing in temperature.
4. Double layer capacitances decrease with respect to blank solution when the inhibitor is added. This fact confirms the adsorption of these molecules on the carbon steel surface.

5. The thermodynamic parameters revealed that the inhibition of corrosion by investigated compounds is due to the formation of a physical adsorbed film on the metal surface.

6. The adsorption of inhibitor on C-steel surface in HCl solution follows Temkin's adsorption for these compounds.

7. The negative values of ΔG°_{ads} indicate spontaneous adsorption of the inhibitors on the surface of C-Steel Surface.

8. The values of inhibition efficiencies obtained from the different independent quantitative techniques used show the validity of the results.

References

- [1] Hosseini, S .M.A., Salari, M., Ghasemi, M., *Mater Corros*, 60 (2009) 963.
- [2] Bilgic, S., Sahin, M., *Mater Chem. Phys*, 70 (2001) 290.
- [3] Lalitha, A., Ramesh, S., Rajeswari, S., *ElectrochimActa*, 51 (2005) 47.
- [4] Sherif, E.M., Park, S.M., *ElectrochimActa*, 51 (2006) 4665.
- [5] Quraishi, M .A., Sardar, R., *Corrosion*, 58 (2002) 103.
- [6] Karakus, M., Sahin, M., Bilgic, S., *Mater ChemPhys*, 92(2005) 565.
- [7] Ashassi-Sorkhabi, H., Ghalebsaz-Jeddi, N., Hashemzadeh, F., Jahani H., *ElectrochimActa*, 51 (2006) 3848.
- [8] S.S.Abdel-Rehim, K.F.Khaled, N.S.Abd-Elshafi, *Electrochim Acta*, 51(2006) 3269.
- [9] Ali, S.A., Saeed, M.T., Rahman, S.U., *CorrosSci*, 45 (2003) 253.
- [10] Yildirim, A., Cetin, M., *CorrosSci*, 50(2008) 155.
- [11] Bartos, M., Hackerman, N., *J ElectrochemSoc*, 139 (1992) 3428.
- [12] Bentiss, F., Lagrenée, M., Traisnel, M. and Hornez, J. C., *J. Corros. Sci*, 41(1999)789-803.
- [13] Bentiss, F., Lagrenée, M. and Traisnel, M., *J. Corros. Sci*, 41 (1999) 625-828.
- [14] Bentiss, F., Traisnel, M. and Lagrenée, M., *J. Appl. Electrochem.*, 31(2001)41-48.
- [15] G.N., Mu, T.P., Zhao, M., Liu, T., GU, *Corrosion*, 52(1996) 853.
- [16] Oguzie, E. E., *Mater. Letters*, 59 (2005) 1076.
- [17] Khaled, K. F., *Mater. Chem. Phys*, 112 (2008) 290-300
- [18] Khaled, K. F., *J. Appl. Electrochem*, 39 (2009) 429-438
- [19] Bosch, R. W., Hubrecht, J., Bogaerts, W. F., Syrett, B. C., *Corrosion*, 57 (2001) 60.
- [20] Abdel-Rehim, S. S., Khaled, K. F., Abd-Elshafi, N. S., *Electrochim. Acta*, 51 (2006) 3269
- [21] Yurt, A., Bereket, G., Kivrak, A., Balaban, A. & Erk, B., *J ApplElectrochem*, 35 (2005) 1025.
- [22] Bentiss, F., Traisnel, M. & Lagrenee, M., *Corros Sci*, 42 (2000) 127.
- [23] Banerjee, G. & Malhotra, S. N., *Corrosion*, 48 (1992) 10.
- [24] Hour, T. P. & Holliday, R. D., *J ApplChem*, 3 (1953) 502.
- [25] Riggs, L. O. (Jr) & Hurd, T. J., *Corrosion*, 23 (1967) 252.
- [26] Schmid, G. M. & Huang, H. J., *CorrosSci*, 20 (1980) 1041.
- [27] Bentiss, F., Lebrini, M. & Lagrenee, M., *Corros. Sci*, 47 (2005) 2915.
- [28] Marsh, J., *Advanced Organic Chemistry*, 3rd edn (Wiley Eastern, New Delhi), (1988).
- [29] Silverman, D. C. and Carrico, J. E., *Corrosion*, 44(1988) 280.
- [30] Lorenz, W. J. and Mansfeld, F., *Corros.Sci*, 21 (1981) 647.
- [31] Macdonald, D. D., Mckubre, M. C., "Impedance measurements in Electrochemical systems," *Modern Aspects of Electrochemistry*, J.O'M. Bockris, B.E. Conway, R.E.White, Eds., Plenum Press, New York, 14(1982)61.
- [32] Mansfeld, F., *Corrosion*, 36(1981) 301.

- [33] Gabrielli, C., "Identification of Electrochemical processes by Frequency Response Analysis," Solartron Instrumentation Group, (1980).
- [34] El Achouri, M., Kertit, S., Gouttaya, H. M., Nciri, B., Bensouda, Y., Perez, L., Infante, M. R., Elkacemi, K., *Prog. Org. Coat*, 43 (2001) 267.
- [35] Macdonald, J.R., Johanson, W.B., in: J.R. Macdonald, (Ed.), *Theory in Impedance Spectroscopy*, John Wiley & Sons, New York, (1987).
- [36] Mertens, S. F., Xhoffer, C., Decooman, B. C., E. Temmerman, *Corrosion*, 53 (1997) 381.
- [37] Trabanelli, G., Montecelli, C., Grassi, V., Frignani, A., *J. Cem. Concr. Res.*, 35 (2005) 1804.
- [38] Trowsdate, A. J., Noble, B., Haris, S. J., Gibbins, I.S. R., Thomson G. E., Wood G. C., *Corros. Sci.*, 38 (1996) 177.
- [39] Reis, F. M., De Melo, H.G. and Costa, I., *Electrochim. Acta*, 51 (2006) 17.
- [40] Lagrenee, M., Mernari, B., Bouanis, M., Traisnel, M. & Bentiss, F., *Corros. Sci.*, 44 (2002) 573.
- [41] McCafferty, E., Hackerman, N., *J. Electrochem. Soc.*, 119 (1972) 146.
- [42] Ma, H., Chen, S., Niu, L., Zhao, S., Li S., Li D., *J. Appl. Electrochem.*, 32 (2002) 65.
- [43] Kus, E., Mansfeld, F., *Corros. Sci.*, 48 (2006) 965.
- [44] Caignan, G. A., Metcalf, S. K., Holt, E. M., *J. Chem. Cryst.*, 30 (2000) 415.
- [45] Schweinsberg, D. P., Graeme, A., George, Nanayakkara, A.K. and Steinert, D.A., *Corros. Sci.*, 28 (1988)